

## Research Article

# An Adaptive $H^\infty$ -Based Formation Control for Multirobot Systems

Faridoon Shabani, Bijan Ranjbar, and Ali Ghadamyari

*School of Electrical Engineering, Shiraz University, Shiraz, Iran*

Correspondence should be addressed to Faridoon Shabani; shabani@shirazu.ac.ir

Received 27 April 2012; Accepted 23 May 2012

Academic Editors: J. B. Koeneman and G. S. Virk

Copyright © 2013 Faridoon Shabani et al. This is an open access article distributed under the Creative Commons Attribution License, which permits unrestricted use, distribution, and reproduction in any medium, provided the original work is properly cited.

We describe a decentralized formation problem for multiple robots, where an  $H^\infty$  formation controller is proposed. The network of dynamic agents with external disturbances and uncertainties are discussed in formation problems. We first describe how to design social potential fields to obtain a formation with the shape of a polygon. Then, we provide a formal proof of the asymptotic stability of the system, based on the definition of a proper Lyapunov function and  $H^\infty$  technique. The advantages of the proposed controller can be listed as robustness to input nonlinearity, external disturbances, and model uncertainties, while applicability on a group of any autonomous systems with  $n$ -degrees of freedom. Finally, simulation results are demonstrated for a multiagent formation problem of a group of six robots, illustrating the effective attenuation of approximation error and external disturbances, even in the case of agent failure or leader tracking.

## 1. Introduction

All around the world, nature presents examples of collective behavior in groups of insects, birds, and fishes. This behavior has produced sophisticated functions of the group that cannot be achieved by individual members [1, 2]. Therefore, the research on the coordination of robotic swarms has attracted considerable attention. Taking the advantages of distributed sensing and actuation, a robotic swarm can perform some cooperative tasks such as moving a large object that is usually not executable by a single robot [3–7]. Applications about the analysis and design of robotic swarms included autonomous unmanned aerial vehicles, congestion control of communication networks, and distributed sensor networks autonomous, and so forth [1, 2, 8–10].

In general, a robotic formation problem is defined as the organization of a swarm of agents into a particular shape in a 2D or 3D space [8]. This kind of control strategy can be applied into several different fields. For example, in the industrial field, this formation control strategy can be applied to a group of Automated Guided Vehicles (AGVs) moving in a warehouse for goods delivery. The main idea is to make a group of AGVs cooperatively deliver a certain

amount of goods, moving in a formation. The creation of a formation with the desired shape is useful to precisely constrain the action zone of the AGVs, thus reducing the chance of collisions with other entities (e.g., human guided vehicles).

In the literature, many different approaches to formation control can be found. The main existing approaches can be divided into two categories: centralized [11] and distributed [12]. Because of the intrinsic unreliability of centralized methods, we focus our attention to distributed ones: all the agents are equal, and if one of them stops working, the other ones can still complete their task. Several formation control strategies can be found as potential fields [8], behavior-based [13], leader-following [14–16], graph-theoretic [12], and virtual structure approaches [17, 18].

In recent years, some methods based on potential fields are integrated with some nonlinear control schemes such as feedback linearization method (e.g., Sliding Mode Control (SMC)), which concludes in more robust formation control designs of dynamic agents [15–18]. For example, Takahashi et al. [15] proposed an SMC-based formation control scheme for multiple mobile robots, using the leader-following strategy, in which they defined some performance

indexes, so that robots can be controlled according to their ability. Defoort et al. [16] also developed a robust coordinated control scheme based on leader-follower approach to achieve formation maneuvers. They used first- and second-order SMC to address the formation problem of  $N$  mobile robots of unicycle type with two driving wheels. Moreover, Cheaha et al. [17] presented a region-based shape controller for a swarm of fully actuated robots, where a linear approximator was used to approximate the unknown dynamic model and an SMC controller integrated with artificial potential functions was used to satisfy a predetermined geometric 2D formation.

Recently,  $H^\infty$  optimal control techniques have been found to be an effective solution to treat robust stabilization and tracking problems, in presence of external disturbances and system uncertainties [19–24]. In an  $H^\infty$  control technique, the main design goal is to force the gain from unmodelled dynamics, external disturbances, and approximation errors to be equal or less than a prescribed disturbance attenuation level ( $H^\infty$  attenuation constraint) [19]. This goal is generally represented as a Linear Matrix Inequality (LMI) problem.

In the traditional  $H^\infty$  control the exact model of the system must be known. However, in order to propose a robust control method, an integration between this robust scheme with fuzzy logic approximators can propose effective controllers for uncertain dynamic models [25].

Since Zadeh [26] initiated the fuzzy set theory, fuzzy logic systems (FLS) have been widely applied to many real world applications [27–30]. However, fuzzy control has not been viewed as a rigorous science due to a lack of formal synthesis techniques which guarantee the very basic requirements of global stability and acceptable performance. In fact, if the mathematical model of a robot is known, then conventional linear and nonlinear approximation methods should be given higher priority. However, fuzzy control should be useful in situations where (1) there is no acceptable mathematical model for the robot and (2) there are experienced human operators who can satisfactorily approximate the plant and provide qualitative control rules in terms of vague and fuzzy sentences. There are many practical situations where both (1) and (2) are true. Besides, FLS schemes have been widely used in motion control of single robots [31, 32]. Using FLS integrated with  $H^\infty$  control technique can improve the robustness of controller and ensures the stability [25].

In this paper, a geometric formation is considered as the goal and an artificial potential is defined to guide the agents through this formation. A partially unknown nonlinear dynamic model is adopted to each  $n$ -degrees of freedom agent. Therefore, an adaptive interval type-2 fuzzy approximator is combined with  $H^\infty$  control technique to propose a novel decentralized adaptive fuzzy formation control methodology, with robust characteristics. The main advantage of this control strategy is insensitivity to robot dynamic uncertainties, external disturbances, and input nonlinearities.

Moreover, in existing adaptive nonlinear control methodologies which are based on SMC control (e.g., [17]), each agent approximator needs to know the position and velocity of all other robots to approximate the unknown model

dynamics; however, in the current proposed decentralized strategy, only the position and velocity of each robot are enough to be known to its approximator.

The rest of this paper is organized as follows: Section 2 presents the system description, problem formulation, and potential function evaluation. An introduction of interval type-2 fuzzy logics systems is described in Section 3. Design of the proposed controller and stability analysis are discussed in Sections 4 and 5, respectively. Simulation results are included in Section 6 and Section 7 provides the concluding remarks.

## 2. System Description and Problem Formulation

The major goal in this study is to solve a multiagent formation control problem (i.e., controlling the relative position and orientation of the agents to create a desirable formation). One of the effective solutions for this problem is using an electrostatic-like potential function design which guides the agents through continues smooth paths and avoids agent collisions. Such a potential function design has been discussed in various papers (e.g., [1, 2, 8, 18]). Therefore, in Section 2.1 we will explain a simple potential function design, in order to solve the formation control of a group of  $N$  point massless agents, where the kinematic of the  $i$ th agent is considered as

$$\dot{z}_i = u_i, \quad i \in \{1, 2, \dots, n\}, \quad (1)$$

in which  $z_i \in R^n$  is the coordinate matrix (for a robot with  $n$ -degrees of freedom) and  $u_i \in R^n$  denotes the control inputs.

However, one of the main shortcomings of this kinematic model is that it does not correspond to the dynamics of realistic agents. To overcome this shortcoming more general dynamic models like unicycle models [33] or other wheeled vehicle models can be discussed.

In Section 2.2 one of the most general  $n$ -degrees of freedom dynamic models of real robots is considered to propose more realistic solutions for formation control of multiagent systems. The main feature of this model is that any agent (robot) with  $n$ -degrees of freedom (e.g., Autonomous Underwater Vehicles (AUVs) [34], Unmanned Aerial Vehicles (UAVs) [35, 36], etc.) can be adopted to this model.

*2.1. Formation Control Massless Agents.* To propose a control law, an artificial potential function is designed. This potential function can be comprised of interagent interactions, environmental effects (e.g., obstacles, goals, etc.), or other exceptional terms.

Consider the pairwise potential fields, which are defined between agents as

$$F_{ij} = L_{ij}(|z_i - z_j|), \quad \forall i, j \in \{1, 2, \dots, n\}, \quad (2)$$

where  $L_{ij}$  is designed to define a proper interagent potential function. It is assumed that each agent senses the resultant potential of all other agents.

The overall potential function is proposed to be in the form of

$$F = \sum_{i=1}^{N-1} \sum_{j=i+1}^N L_{ij} (|z_i - z_j|) + \sum_{i=1}^N Q_i (|z_i|), \quad (3)$$

where  $Q_i$  defines the global potential of each agent.

Finally, the following three assumptions for potential function are considered [17, 18].

*Assumption 1.*  $F$  is continuously differentiable.

*Assumption 2.*  $F$  is strictly convex.

*Assumption 3.*  $F$  is positive definite.

For example, the following potential function can be chosen for a desired polygonal formation in a 2D Space:

$$F = \sum_{i=1}^{N-1} \sum_{j=i+1}^N (|z_i - z_j|^2 - d_{ij})^2 + \sum_{i=1}^N (|z_i|^2 - r_i)^2. \quad (4)$$

At the first step, to propose a solution for multiagent formation control, the steepest descent direction [8, 17, 18] is chosen as

$$f_i = \frac{\partial F}{\partial z_i}, \quad (5)$$

and the control law

$$u_i = -f_i, \quad \forall i \in \{1, 2, \dots, n\} \quad (6)$$

is proposed.

By substituting (6) in (1) the kinematic model is obtained as

$$\dot{z}_i = -f_i = -\frac{\partial F}{\partial z_i}, \quad \forall i \in \{1, 2, \dots, n\}, \quad (7)$$

which can be rewritten in the matrix form as  $\dot{Z} = -\nabla F$  where  $Z = [z_1, z_2, \dots, z_n]$  is the overall generalized coordinate vector.

In the next subsection, it is proposed to assume the multiagent system with a general dynamic model. Furthermore, in Section 3 a robust adaptive fuzzy controller using an  $H^\infty$  approach is used to force the satisfaction of (7). In other words the proposed controller is designed to enforce the speed of each agent along the negative gradient of potential function in (7).

**2.2. Formation Control of Robots with Dynamic Models.** In this subsection a general dynamic model [37] is addressed to represent any kind of autonomous  $n$ -degrees of freedom system. This model has been previously used in some existing works (e.g., [17, 18]).

Consider a group of  $N$  fully autonomous agents. The dynamics of the  $i$ th simple agent is strongly nonlinear [37] and can be written in the general form

$$M(z_i) \ddot{z}_i + C(z_i, \dot{z}_i) \dot{z}_i + g(z_i) = u_i, \quad (8)$$

where  $z_i \in R^n$  is the coordinate matrix (for a robot with  $n$ -degrees of freedom);  $M(z_i) \in R^{n \times n}$  is a symmetric positive definite matrix and represents the inertia coefficients.  $C(z_i, \dot{z}_i) \in R^{n \times n}$  is the matrix of centripetal, Coriolis, damping, and rolling resistance forces;  $g(z_i) \in R^n$  is an  $n$ -vector of gravitational forces and  $u_i \in R^n$  denotes the control inputs.

In most practical control problems of multiagent systems the inertia matrix  $M(z_i)$  is a known constant matrix independent of  $z_i$ . Therefore, the following assumption is considered.

*Assumption 4.*  $M$  is the inertia matrix of robots, which is assumed to be a known and constant matrix.

Let us rewrite (8) as

$$M\ddot{z}_i + C(z_i, \dot{z}_i) \dot{z}_i + g(z_i) = u_i. \quad (9)$$

It is straightforward to rewrite (9) as

$$\ddot{z}_i = -M^{-1}C(z_i, \dot{z}_i) \dot{z}_i - M^{-1}g(z_i) + M^{-1}u_i. \quad (10)$$

In the next sections, the dynamic of each single agent will be assumed to be in the form of (10).

### 3. Interval Type-2 Fuzzy Logic System

In this section, the interval type-2 fuzzy set and the inference of the type-2 fuzzy logic system will be presented. A type-2 fuzzy set in universal set  $X$  is denoted as  $\tilde{A}$  which is characterized by a type-2 membership function  $u_{\tilde{A}}(x)$  in (12). The  $u_{\tilde{A}}(x)$  can be referred to as a secondary membership function or referred to as a secondary set, which is a type-1 fuzzy set in  $[0, 1]$ . In (13),  $f_x(u)$  is a secondary grade, which is the amplitude of a secondary membership function; that is,  $0 \leq f_x(u) \leq 1$ . The domain of a secondary membership function is called the primary membership of  $x$ . In (13),  $J_x$  is the primary membership of  $x$ , where  $u \in J_x \subseteq [0, 1]$  for all  $x \in X$ ;  $\mu$  is a fuzzy set in  $[0, 1]$ , rather than a crisp point in  $[0, 1]$ ,

$$\tilde{A} = \int_{x \in X} \frac{u_{\tilde{A}}(x)}{x} = \int_{x \in X} \frac{\left[ \int_{u \in J_x} f_x(u) / u \right]}{x}, \quad J_x \subseteq [0, 1]. \quad (11)$$

When  $f_x(u) = 1$ , for all  $u \in J_x \subseteq [0, 1]$ , then the secondary MFs are interval sets such that  $u_{\tilde{A}}(x)$  in (13) can be called an interval type-2 MF. Therefore, the type-2 fuzzy set can be rewritten as

$$\tilde{A} = \int_{x \in X} \frac{u_{\tilde{A}}(x)}{x} = \int_{x \in X} \frac{\left[ \int_{u \in J_x} 1/u \right]}{x}, \quad J_x \subseteq [0, 1]. \quad (12)$$

Also, a Gaussian primary MF with uncertain mean and fixed standard deviation having an interval type-2 secondary MF can be called an interval type-2 Gaussian MF (13). It can be expressed as

$$u_{\tilde{A}}(x) = \exp \left[ -\frac{1}{2} \left( \frac{x - m}{\sigma} \right)^2 \right], \quad m \in [m_1, m_2]. \quad (13)$$

It is obvious that the type-2 fuzzy set is in a region, called a footprint of uncertainty (FOU) and is bounded by an upper MF and a lower MF, which are denoted as  $\bar{u}_{\bar{A}}(x)$  and  $\underline{u}_{\bar{A}}(x)$ , respectively. Hence, (13) can be reexpressed as

$$\bar{A} = \int_{x \in X} \frac{\left[ \int_{u \in [\underline{u}_{\bar{A}}(x), \bar{u}_{\bar{A}}(x)]} 1/u \right]}{x}. \quad (14)$$

A type-2 fuzzy logic system (FLS) is very similar to a type-1 FLS as shown in Figure 1; the major structure difference being that the defuzzifier block of a type-1 FLS is replaced by the output processing block in a type-2 FLS which consists of type-reduction followed by defuzzification.

There are five main parts in a type-2 FLS: fuzzifier, rule base, inference engine, type reducer, and defuzzifier. A type-2 FLS is a mapping  $f : \mathbb{R}^p \rightarrow \mathbb{R}^1$ . After defuzzification, fuzzy inference, type reduction, and defuzzification, a crisp output can be obtained.

Consider a type-2 FLS having  $p$  inputs  $x_1 \in X_1, \dots, x_p \in X_p$  and one output  $y \in Y$ . The type-2 fuzzy rule base consists of a collection of IF-THEN rules, as in the type-1 case. We assume there are  $M$  rules and the rule of a type-2 relation between the input space  $X_1 \times X_2 \times \dots \times X_p$  and the output space  $Y$  can be expressed as

$$R^l : \text{IF } x_1 \text{ is } \bar{F}_1^l \text{ and } \dots \text{ and } x_p \text{ is } \bar{F}_p^l, \text{ THEN } y \text{ is } \bar{G}^l, \quad (15)$$

$$l = 1, 2, \dots, M,$$

where  $\bar{F}_j^l$  are antecedent type-2 sets ( $j = 1, 2, \dots, p$ ) and  $\bar{G}^l$  is consequent type-2 sets.

The inference engine combines rules and gives a mapping from input type-2 fuzzy sets to output type-2 fuzzy sets. To achieve this process, we have to compute unions and intersection of type-2 sets, as well as compositions of type-2 relations. The output of inference engine block is a type-2 set. By using the extension principle of type-1 defuzzification method, type-reduction takes us from type-2 output sets of the FLS to a type-1 set called the "type-reduced set." This set may then be defuzzified to obtain a single crisp value.

There are many kinds of type-reduction, such as centroid, height, modified weight, and center-of-sets. The center-of-sets type reduction will be used in this paper and can be expressed as:

$$Y_{\cos} (Y^1, \dots, Y^M, F^1, \dots, F^M) = [y_l, y_r]$$

$$= \int_{y_l} \dots \int_{y_r} \int_{f^1} \dots \int_{f^M} \frac{1}{\sum_{i=1}^M f^i y^i / \sum_{i=1}^M f^i}, \quad (16)$$

where  $Y_{\cos}$  is the interval set determined by two end points  $y_l$  and  $y_r$ , and  $f^i \in F^i = [\underline{f}^i, \bar{f}^i]$ . In the meantime, an interval type-2 FLS with singleton fuzzification and meet under minimum or product t-norm  $\underline{f}^i$  and  $\bar{f}^i$  can be obtained as

$$\underline{f}^i = \underline{\mu}_{\bar{F}_1^i}(x_1) * \dots * \underline{\mu}_{\bar{F}_p^i}(x_p), \quad (17)$$

$$\bar{f}^i = \bar{\mu}_{\bar{F}_1^i}(x_1) * \dots * \bar{\mu}_{\bar{F}_p^i}(x_p). \quad (18)$$

Also,  $y^i \in Y^i$  and  $Y^i = [y_l^i, y_r^i]$  are the centroid of the type-2 interval consequent set  $\bar{G}^i$ . For any value  $y \in Y_{\cos}$ ,  $y$  can be expressed as

$$y = \frac{\sum_{i=1}^M f^i y^i}{\sum_{i=1}^M f^i}, \quad (19)$$

where  $y$  is a monotonic increasing function with respect to  $y^i$ . Also,  $y_l$  is the minimum associated only with  $y_l^i$ , and  $y_r$  is the maximum associated only with  $y_r^i$ . Note that  $y_l$  and  $y_r$  depend only on mixture of  $\underline{f}^i$  or  $\bar{f}^i$  values. Therefore, the left-most point  $y_l$  and the right-most point  $y_r$  can be expressed as a fuzzy basis function (FBF) expansion, that is,

$$y_l = \frac{\sum_{i=1}^M f_l^i y_l^i}{\sum_{i=1}^M f_l^i} = \sum_{i=1}^M y_l^i \xi_l^i, \quad (20)$$

$$y_r = \frac{\sum_{i=1}^M f_r^i y_r^i}{\sum_{i=1}^M f_r^i} = \sum_{i=1}^M y_r^i \xi_r^i,$$

respectively, where  $\xi_l^i = f_l^i / \sum_{i=1}^M f_l^i$  and  $\xi_r^i = f_r^i / \sum_{i=1}^M f_r^i$ .

If the FBF vector denoted as  $\xi_{\underline{l}} = [\xi_l^1, \xi_l^2, \dots, \xi_l^M]$  and  $\xi_{\underline{r}} = [\xi_r^1, \xi_r^2, \dots, \xi_r^M]$ , and let  $\underline{y}_l^T = [y_l^1, y_l^2, \dots, y_l^M]$  and  $\underline{y}_r^T = [y_r^1, y_r^2, \dots, y_r^M]$ , then (20) can be rewritten as

$$y_l = \frac{\sum_{i=1}^M f_l^i y_l^i}{\sum_{i=1}^M f_l^i} = \sum_{i=1}^M y_l^i \xi_l^i = \underline{y}_l^T \xi_{\underline{l}}, \quad (21)$$

$$y_r = \frac{\sum_{i=1}^M f_r^i y_r^i}{\sum_{i=1}^M f_r^i} = \sum_{i=1}^M y_r^i \xi_r^i = \underline{y}_r^T \xi_{\underline{r}}. \quad (22)$$

For illustrative purposes, we briefly provide the computation procedure for  $y_r$ . Without loss of generality, assume the  $y_r^i$ s are arranged in ascending order, that is,  $y_r^1 \leq y_r^2 \leq \dots \leq y_r^M$ .

*Step 1.* Compute  $y_r$  in (22) by initially setting  $f_r^i = (\bar{f}^i + \underline{f}^i)/2$  for  $i = 1, 2, \dots, M$ , where  $\underline{f}^i$  and  $\bar{f}^i$  have been precomputed by (18) and (19) and let  $y_r^i = y_r$ .

*Step 2.* Find  $R$  ( $1 \leq R \leq M - 1$ ) such that  $y_r^R \leq y_r^i \leq y_r^{R+1}$ .

*Step 3.* Compute  $y_r$  in (22) with  $f_r^i = \underline{f}^i$  for  $i \leq R$  and  $f_r^i = \bar{f}^i$  for  $i > R$  and let  $y_r^{i'} = y_r$ .

*Step 4.* If  $y_r^{i'} \neq y_r^i$ , then go to Step 5, If  $y_r^{i'} = y_r^i$ , then stop and set  $y_r = y_r^{i'}$ .

*Step 5.* Set  $y_r^i$  equal to  $y_r^{i'}$  and return to Step 2.

The point to separate two sides by number  $R$  can be decided from the above algorithm, one side using lower firing

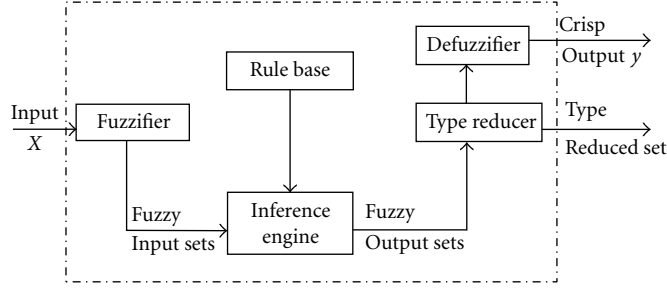


FIGURE 1: The structure of the type-2 fuzzy logic system.

strengths  $\underline{f}^i$ 's and another side using upper firing strengths  $\bar{f}^i$ 's. Therefore, the  $y_r$  in (22) can be rewritten as

$$\begin{aligned} y_r &= \frac{\sum_{i=1}^R \underline{f}^i y_r^i + \sum_{i=R+1}^M \bar{f}^i y_r^i}{\sum_{i=1}^R \underline{f}^i + \sum_{i=R+1}^M \bar{f}^i} = \sum_{i=1}^R \underline{q}_r^i y_r^i + \sum_{i=R+1}^M \bar{q}_r^i y_r^i \\ &= \begin{bmatrix} \underline{Q}_r & \bar{Q}_r \end{bmatrix} \begin{bmatrix} y_r \\ \bar{y}_r \end{bmatrix} = \xi_r^T \Theta_r, \end{aligned} \quad (23)$$

where  $\underline{q}_r^i = \underline{f}^i / D_r$ ,  $\bar{q}_r^i = \bar{f}^i / D_r$  and  $D_r = (\sum_{i=1}^R \underline{f}^i + \sum_{i=R+1}^M \bar{f}^i)$ . In the meantime, we have  $\underline{Q}_r = [q_r^1, q_r^2, \dots, q_r^R]$ ,  $\bar{Q}_r = [\bar{q}_r^1, \bar{q}_r^2, \dots, \bar{q}_r^R]$ ,  $\xi_r^T = [\underline{Q}_r \quad \bar{Q}_r]$ , and  $\Theta_r^T = [y_r \quad \bar{y}_r]$ .

The procedure to compute  $y_l$  is similar to compute  $y_r$ . Just in Step 2, we determine  $L$  ( $1 \leq L \leq M - 1$ ), such that  $y_l^L \leq y_l^i \leq y_l^{L+1}$  and in Step 3 let  $f_l^i = \bar{f}^i$  for  $i \leq L$  and  $f_l^i = \underline{f}^i$  for  $i > L$ . Then  $y_l$  in (21) can also be rewritten as

$$\begin{aligned} y_l &= \frac{\sum_{i=1}^L \bar{f}^i y_l^i + \sum_{i=L+1}^M \underline{f}^i y_l^i}{\sum_{i=1}^L \bar{f}^i + \sum_{i=L+1}^M \underline{f}^i} = \sum_{i=1}^L \bar{q}_l^i y_l^i + \sum_{i=L+1}^M \underline{q}_l^i y_l^i \\ &= \begin{bmatrix} \bar{Q}_l & \underline{Q}_l \end{bmatrix} \begin{bmatrix} \bar{y}_l \\ y_l \end{bmatrix} = \xi_l^T \Theta_l, \end{aligned} \quad (24)$$

where  $\underline{q}_l^i = \underline{f}^i / D_l$ ,  $\bar{q}_l^i = \bar{f}^i / D_l$  and  $D_l = (\sum_{i=1}^L \bar{f}^i + \sum_{i=L+1}^M \underline{f}^i)$ . In the meantime, we have  $\underline{Q}_l = [q_l^1, q_l^2, \dots, q_l^R]$ ,  $\bar{Q}_l = [\bar{q}_l^1, \bar{q}_l^2, \dots, \bar{q}_l^R]$ ,  $\xi_l^T = [\bar{Q}_l \quad \underline{Q}_l]$ , and  $\Theta_l^T = [\bar{y}_l \quad y_l]$ .

The defuzzified crisp value from an interval type-2 FLS is obtained as

$$\begin{aligned} y(x) &= \frac{y_l + y_r}{2} = \frac{1}{2} (\xi_r^T \Theta_r + \xi_l^T \Theta_l) \\ &= \frac{1}{2} \begin{bmatrix} \xi_r^T & \xi_l^T \end{bmatrix} \begin{bmatrix} \Theta_r \\ \Theta_l \end{bmatrix} = \xi^T \Theta, \end{aligned} \quad (25)$$

where  $(1/2) [\xi_r^T \quad \xi_l^T] = \xi^T$  and  $[\Theta_r^T \quad \Theta_l^T] = \Theta^T$ .

## 4. Controller Design Methodology

In this section a novel formation error based on the integral of formation gradient (5) will be proposed. Then, a robust  $H^\infty$  controller will be designed and a fuzzy logic system will be utilized to approximate the unknown parts of dynamic models. The main feature of the proposed novel control scheme is its decentralized characteristic, robustness to external disturbances, input nonlinearities, and measurement noises. Besides, by using the proposed controller, the formation can be achieved from any initial conditions.

Consider, the novel formation error for the  $i$ th robot as

$$\underline{e}_i(t) = z_i(t) + \int_0^t f_i(\tau) d\tau, \quad (26)$$

where  $e_i \in R^n$ ,  $z_i$  represents the coordinate vector of  $i$ th robot in (10) and  $f_i$  is the gradient of potential function defined in (7). It is straightforward to write the first and second derivatives of (26) as

$$\dot{\underline{e}}_i(t) = \dot{z}_i(t) + f_i, \quad (27)$$

$$\ddot{\underline{e}}_i(t) = \ddot{z}_i(t) + \dot{f}_i.$$

Our design goal is to propose an adaptive fuzzy controller so that

$$\ddot{\underline{e}}_i + k_1 \dot{\underline{e}}_i + k_2 \underline{e}_i = 0 \quad (28)$$

is achieved, where  $k_1$  and  $k_2$  are chosen to make (28) asymptotically stable.

To design the controller, consider the control law proposed as

$$u_i = M (H_i(z_i, \dot{z}_i) - \dot{f}_i - k_1 \dot{\underline{e}}_i - k_2 \underline{e}_i), \quad (29)$$

where

$$H_i(z_i, \dot{z}_i) = M^{-1} C_i(z_i, \dot{z}_i) \dot{z}_i + M^{-1} g(z_i). \quad (30)$$

In order to use this control law, which is designed based on the feedback linearization control method, the function  $H_i(\cdot)$  (i.e.,  $C(\cdot)$  and  $g(\cdot)$ ) must be known. However, in practice these matrices may be unknown for most of real dynamical robots. To overcome this, we make use of an adaptive fuzzy logic system  $\widehat{H}_i(\cdot)$  to approximate  $H_i(\cdot)$ .

Therefore, using the singleton fuzzifier, product inference, and weighted average defuzzifier [38], the output of the fuzzy model can be expressed as

$$\widehat{H}_i(z_i, \dot{z}_i | \underline{\theta}_i) = \frac{1}{2} \left( \zeta_{il}^T(z_i, \dot{z}_i) \underline{\theta}_{il} + \zeta_{ir}^T(z_i, \dot{z}_i) \underline{\theta}_{ir} \right), \quad (31)$$

where

$$\zeta_{il} = \begin{bmatrix} \zeta_{1il}^T & 0 & \cdots & 0 \\ 0 & \zeta_{2il}^T & \cdots & 0 \\ \vdots & \vdots & \ddots & \vdots \\ 0 & 0 & \cdots & \zeta_{nil}^T \end{bmatrix}, \quad \underline{\theta}_{il} = \begin{bmatrix} \theta_{1il} \\ \theta_{2il} \\ \vdots \\ \theta_{nil} \end{bmatrix}, \quad (32)$$

$$\zeta_{ir} = \begin{bmatrix} \zeta_{1ir}^T & 0 & \cdots & 0 \\ 0 & \zeta_{2ir}^T & \cdots & 0 \\ \vdots & \vdots & \ddots & \vdots \\ 0 & 0 & \cdots & \zeta_{nir}^T \end{bmatrix}, \quad \underline{\theta}_{ir} = \begin{bmatrix} \theta_{1ir} \\ \theta_{2ir} \\ \vdots \\ \theta_{nir} \end{bmatrix}.$$

Equation (31) suggests to us to rewrite the overall control law (29) as

$$u_i = M \left( \widehat{H}_i(z_i, \dot{z}_i | \underline{\theta}_i) - \dot{f}_i - k^T \underline{e}_i - \underline{u}_{ai} \right), \quad (33)$$

where  $u_{ai}$  is engaged to attenuate the fuzzy logic approximation error and external disturbances.

A block diagram of the proposed control methodology is shown in Figure 2.

*Remark 1 (input nonlinearity).* In what follows, another main property of the proposed  $H^\infty$  is introduced. It will be shown that the formation problem of multiagent system can be achieved even in the presence of dead-zone nonlinearities of the control actuators. Let us modify the dynamic model (9) as

$$M\ddot{z}_i + C(z_i, \dot{z}_i) \dot{z}_i + g(z_i) = \Phi(u_i) + d_i(t) \quad (34)$$

where

$$\Phi(u_i) = \begin{bmatrix} \phi(u_{i1}) \\ \phi(u_{i2}) \\ \vdots \\ \phi(u_{in}) \end{bmatrix} \quad (35)$$

and  $\phi(\cdot) : R \rightarrow R$  represents the dead-zone function and can be expressed as

$$\phi(u) = \begin{cases} m(u - b) & u \geq b, \\ 0 & -b < u < b, \\ m(u + b) & u \leq -b, \end{cases} \quad (36)$$

where  $b$  is the width of the dead-zone and  $m$  is the slope of dead-zone line.

The dead-zone parameters  $b$  and  $m$  are assumed to be bounded and the bounds of  $m$  and  $b$  are known as  $b \in [b_{\min}, b_{\max}]$  and  $m \in [m_{\min}, m_{\max}]$ . Therefore (36) can be rewritten as

$$\phi(u) = mu + v(u),$$

$$v(u) = \begin{cases} -mb & u \geq b, \\ -mu & -b < u < b, \\ mb & u \leq -b. \end{cases} \quad (37)$$

From the aforementioned assumption on bounds of  $m$  and  $b$ ,  $v(u)$  can be assumed bounded, (i.e.,  $v(u) \leq \rho$ ), where  $\rho$  is the known upper bound that can be chosen as  $\rho = mb_{\max}$ . By considering  $\bar{d}_i(t) = d_i(t) + Y(u_i)$  and  $\bar{u}_i = Mu_i$ , where

$$Y(u_i) = \begin{bmatrix} v_1(u_{i1}) \\ v_2(u_{i2}) \\ \vdots \\ v_n(u_{in}) \end{bmatrix}, \quad M = mI_{n \times n} \quad (38)$$

then (34) can be rewritten as

$$M\ddot{z}_i + C(z_i, \dot{z}_i) \dot{z}_i + g(z_i) = \bar{u}_i + \bar{d}_i(t), \quad (39)$$

which is the same as (9). Therefore, we have proved that the proposed  $H^\infty$  feedback controller is also robust to dead-zone input nonlinearities (36).

## 5. Stability Analysis

This section presents the stability proof of the proposed novel adaptive fuzzy controller in (33). A Lyapunov candidate will be proposed and then an adaptation law and a robust compensator control input will be derived to satisfy the  $H^\infty$  tracking performance in (50).

To derive the adaptive law for adjusting  $\underline{\theta}_i$ , we first define the optimal parameter vector  $\underline{\theta}_i^*$  as

$$\underline{\theta}_i^* = \arg \min_{\underline{\theta}_i \in \Omega} \left[ \sup \| \widehat{H}_i(z, \dot{z} | \underline{\theta}_i) - H_i(z, \dot{z}) \| \right], \quad (40)$$

and the minimum approximation error is defined as

$$\underline{w}_i = H_i(z_i, \dot{z}_i) - \widehat{H}_i(z_i, \dot{z}_i | \underline{\theta}_i^*), \quad (41)$$

where it can be assumed that  $\underline{w}_i \in L_\infty$  [38].

By choosing the control input as [39] after some manipulations, (10) can be rewritten as

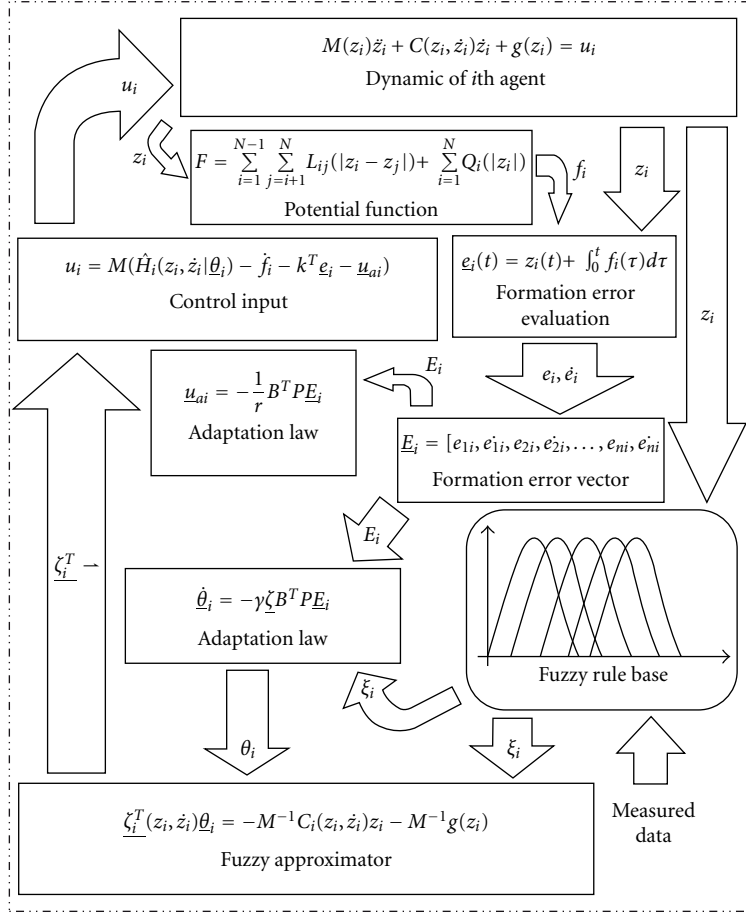
$$\ddot{z}_i + \dot{f}_i = \left( \widehat{H}_i(z_i, \dot{z}_i | \underline{\theta}_i) - H_i(z_i, \dot{z}_i) \right) + k_1 \dot{e}_i + k_2 e_i - \underline{u}_{ai}, \quad (42)$$

and the formation error dynamic can be expressed as

$$\ddot{e}_i = \left( \widehat{H}_i(z_i, \dot{z}_i | \underline{\theta}_i) - H_i(z_i, \dot{z}_i) \right) + k_1 \dot{e}_i + k_2 e_i - \underline{u}_{ai}. \quad (43)$$

Moreover by defining  $\underline{E}_i = [e_{1i}, \dot{e}_{1i}, e_{2i}, \dot{e}_{2i}, \dots, e_{ni}, \dot{e}_{ni}]$  it is straightforward to write

$$\dot{\underline{E}}_i = A \underline{E}_i + B \underline{u}_{ai} + B \left( H_i(z_i, \dot{z}_i) - \widehat{H}_i(z_i, \dot{z}_i | \underline{\theta}_i) \right), \quad (44)$$


 FIGURE 2: Block diagram of the proposed adaptive fuzzy  $H^\infty$  control scheme.

where

$$A = I_{n \times n} \otimes \begin{bmatrix} 0 & 1 \\ -k_2 & -k_1 \end{bmatrix}_{2 \times 2}, \quad B = I_{n \times n} \otimes [0 \ 1]^T. \quad (45)$$

Based on (31), (40), and (41), the matrix form of formation error in (44) can be rewritten as

$$\dot{\underline{E}}_i = A \underline{E}_i + B \underline{u}_{ai} + B \zeta_i^T(z_i, \dot{z}_i) \tilde{\theta}_i + B \underline{w}_i, \quad (46)$$

where  $\tilde{\theta}_i = \theta_i - \theta_i^*$ .

In the following theorem, it will be shown that the proposed control law (33) guarantees the stability and robustness of formation problem.

**Theorem 2.** Consider a group of  $N$  fully autonomous agents with the dynamic represented in (8) and with the control law in (33). The robust compensator of  $i$ th robot  $\underline{u}_{ai}$  and the fuzzy adaptation law are chosen as

$$\underline{u}_{ai} = -\frac{1}{r} B^T P \underline{E}_i, \quad (47)$$

$$\dot{\underline{\theta}}_{il} = -\gamma \zeta_{il}(z_i, \dot{z}_i) B^T P \underline{E}_i, \quad \dot{\underline{\theta}}_{ir} = -\gamma \zeta_{ir}(z_i, \dot{z}_i) B^T P \underline{E}_i, \quad (48)$$

where  $r$  and  $\gamma$  are positive constants and  $P$  is the positive semidefinite solution of following Riccati-like equation:

$$PA + A^T P + Q - \frac{2}{r} P B B^T P + \frac{1}{\rho^2} P B B^T P = 0, \quad (49)$$

where  $Q$  is a positive semidefinite matrix and  $2\rho^2 \geq r$ .

Therefore, the  $H^\infty$  tracking performance

$$\begin{aligned} & \sum_{i=1}^N \left[ -\int_0^T \underline{E}_i^T Q \underline{E}_i dt \right] \\ & \leq \sum_{i=1}^N \left[ \underline{E}_i(0)^T P \underline{E}_i(0) + \frac{1}{2\gamma} \tilde{\theta}_{il}(0)^T \tilde{\theta}_{il}(0) + \frac{1}{2\gamma} \tilde{\theta}_{ir}(0)^T \tilde{\theta}_{ir}(0) \right] \\ & \quad + \sum_{i=1}^N \left[ \rho^2 \int_0^T \underline{w}_i^T \underline{w}_i dt \right] \end{aligned} \quad (50)$$

can be achieved for a prescribed attenuation level  $\rho$  and all the variables of closed loop system are bounded.

In order to derive the adaptive law for adjusting  $\underline{\theta}_i$ , the Lyapunov candidate is chosen as

$$V = \sum_{i=1}^N \left[ \frac{1}{2} \underline{E}_i^T P \underline{E}_i + \frac{1}{4\gamma} \underline{\tilde{\theta}}_{il}^T \underline{\tilde{\theta}}_{il} + \frac{1}{4\gamma} \underline{\tilde{\theta}}_{ir}^T \underline{\tilde{\theta}}_{ir} \right]. \quad (51)$$

Using (46), the time derivative of  $V$  is

$$\begin{aligned} \dot{V} &= \frac{1}{2} \sum_{i=1}^N \left[ \dot{\underline{E}}_i^T P \underline{E}_i + \underline{E}_i^T P \dot{\underline{E}}_i + \frac{1}{2\gamma} \dot{\underline{\tilde{\theta}}}_{il}^T \underline{\tilde{\theta}}_{il} + \frac{1}{2\gamma} \underline{\tilde{\theta}}_{il}^T \dot{\underline{\tilde{\theta}}}_{il} \right. \\ &\quad \left. + \frac{1}{2\gamma} \dot{\underline{\tilde{\theta}}}_{ir}^T \underline{\tilde{\theta}}_{ir} + \frac{1}{2\gamma} \underline{\tilde{\theta}}_{ir}^T \dot{\underline{\tilde{\theta}}}_{ir} \right] \\ &= \frac{1}{2} \sum_{i=1}^N \left[ \underline{E}_i^T A^T P \underline{E}_i + \underline{u}_{ai}^T B^T P \underline{E}_i + \frac{1}{2} \underline{\tilde{\theta}}_{il}^T \underline{\zeta}_{il}(z_i, \dot{z}_i) B^T P \underline{E}_i \right. \\ &\quad \left. + \frac{1}{2} \underline{\tilde{\theta}}_{ir}^T \underline{\zeta}_{ir}(z_i, \dot{z}_i) B^T P \underline{E}_i + \underline{w}_i^T B^T P \underline{E}_i + \underline{E}_i^T P A \underline{E}_i \right. \\ &\quad \left. + \underline{E}_i^T P B \underline{u}_{ai} + \frac{1}{2} \underline{E}_i^T P B \underline{\zeta}_{il}^T(z_i, \dot{z}_i) \underline{\tilde{\theta}}_{il} \right. \\ &\quad \left. + \underline{E}_i^T P B \underline{\zeta}_{ir}^T(z_i, \dot{z}_i) \underline{\tilde{\theta}}_{ir} + \underline{E}_i^T P B \underline{w}_i \right] \\ &\quad + \frac{1}{4} \sum_{i=1}^N \left[ \frac{1}{\gamma} \dot{\underline{\tilde{\theta}}}_{il}^T \underline{\tilde{\theta}}_{il} + \frac{1}{\gamma} \underline{\tilde{\theta}}_{il}^T \dot{\underline{\tilde{\theta}}}_{il} + \frac{1}{\gamma} \dot{\underline{\tilde{\theta}}}_{ir}^T \underline{\tilde{\theta}}_{ir} + \frac{1}{\gamma} \underline{\tilde{\theta}}_{ir}^T \dot{\underline{\tilde{\theta}}}_{ir} \right]. \end{aligned} \quad (52)$$

Substituting (47) in (52) and using the fact that  $\dot{\underline{\tilde{\theta}}}_{il} = \underline{\dot{\theta}}_{il}$ ,  $\dot{\underline{\tilde{\theta}}}_{ir} = \underline{\dot{\theta}}_{ir}$ , we get

$$\begin{aligned} \dot{V} &= \frac{1}{2} \sum_{i=1}^N \left[ \underline{E}_i^T A^T P \underline{E}_i - \frac{1}{r} \underline{E}_i^T P B B^T P \underline{E}_i + \frac{1}{2} \underline{\tilde{\theta}}_{il}^T \underline{\zeta}_{il}(z_i, \dot{z}_i) B^T P \underline{E}_i \right. \\ &\quad \left. + \frac{1}{2} \underline{\tilde{\theta}}_{ir}^T \underline{\zeta}_{ir}(z_i, \dot{z}_i) B^T P \underline{E}_i + \underline{w}_i^T B^T P \underline{E}_i \right. \\ &\quad \left. + \underline{E}_i^T P A \underline{E}_i - \frac{1}{r} \underline{E}_i^T P B B^T P \underline{E}_i + \frac{1}{2} \underline{E}_i^T P B \underline{\zeta}_{il}^T(z_i, \dot{z}_i) \underline{\tilde{\theta}}_{il} \right. \\ &\quad \left. + \frac{1}{2} \underline{E}_i^T P B \underline{\zeta}_{ir}^T(z_i, \dot{z}_i) \underline{\tilde{\theta}}_{ir} + \underline{E}_i^T P B \underline{w}_i \right] \\ &\quad + \frac{1}{4} \sum_{i=1}^N \left[ \frac{1}{\gamma} \underline{\dot{\theta}}_{il}^T \underline{\tilde{\theta}}_{il} + \frac{1}{\gamma} \underline{\tilde{\theta}}_{il}^T \underline{\dot{\theta}}_{il} + \frac{1}{\gamma} \underline{\dot{\theta}}_{ir}^T \underline{\tilde{\theta}}_{ir} + \frac{1}{\gamma} \underline{\tilde{\theta}}_{ir}^T \underline{\dot{\theta}}_{ir} \right] \\ &\quad \times \frac{1}{2} \sum_{i=1}^N \left[ \underline{E}_i^T \left( A^T P + P A - \frac{2}{r} P B B^T P \right) \underline{E}_i \right] \\ &\quad + \frac{1}{4} \sum_{i=1}^N \left[ \left( \underline{E}_i^T P B \underline{\zeta}_{il}^T(z_i, \dot{z}_i) + \frac{1}{\gamma} \underline{\dot{\theta}}_{il}^T \right) \underline{\tilde{\theta}}_{il} \right] \end{aligned}$$

$$\begin{aligned} &+ \frac{1}{4} \sum_{i=1}^N \left[ \left( \underline{E}_i^T P B \underline{\zeta}_{ir}^T(z_i, \dot{z}_i) + \frac{1}{\gamma} \underline{\dot{\theta}}_{ir}^T \right) \underline{\tilde{\theta}}_{ir} \right] \\ &+ \frac{1}{2} \sum_{i=1}^N \left[ \underline{w}_i^T B^T P \underline{E}_i + \underline{E}_i^T P B \underline{w}_i \right]. \end{aligned} \quad (53)$$

Using adaptation law (48) and the Riccati-like equation (49), the above equation becomes

$$\begin{aligned} \dot{V} &= \frac{1}{2} \sum_{i=1}^N \left[ -\underline{E}_i^T Q \underline{E}_i - \frac{1}{\rho^2} \underline{E}_i^T P B B^T P \underline{E}_i \right] \\ &\quad + \frac{1}{2} \sum_{i=1}^N \left[ \underline{w}_i^T B^T P \underline{E}_i + \underline{E}_i^T P B \underline{w}_i \right] \\ &\quad \times \frac{1}{2} \sum_{i=1}^N \left[ -\underline{E}_i^T Q \underline{E}_i - \left( \frac{1}{\rho} B^T P \underline{E}_i - \rho \underline{w}_i \right)^T \left( \frac{1}{\rho} B^T P \underline{E}_i - \rho \underline{w}_i \right) \right] \\ &\quad + \frac{1}{2} \sum_{i=1}^N \left[ \rho^2 \underline{w}_i^T \underline{w}_i \right] \leq \frac{1}{2} \sum_{i=1}^N \left[ -\underline{E}_i^T Q \underline{E}_i + \rho^2 \underline{w}_i^T \underline{w}_i \right]. \end{aligned} \quad (54)$$

Integrating the above inequality from  $t = 0$  to  $T$  yields to

$$V(T) - V(0) \leq \frac{1}{2} \sum_{i=1}^N \left[ - \int_0^T \underline{E}_i^T Q \underline{E}_i dt + \rho^2 \int_0^T \underline{w}_i^T \underline{w}_i dt \right]. \quad (55)$$

Using the fact that  $V(T) \geq 0$  and from (49), the inequality

$$\begin{aligned} &\frac{1}{2} \sum_{i=1}^N \left[ - \int_0^T \underline{E}_i^T Q \underline{E}_i dt \right] \\ &\leq \frac{1}{2} \sum_{i=1}^N \left[ \underline{E}_i(0)^T P \underline{E}_i(0) + \frac{1}{2\gamma} \underline{\tilde{\theta}}_{il}(0)^T \underline{\tilde{\theta}}_{il}(0) + \frac{1}{2\gamma} \underline{\tilde{\theta}}_{ir}(0)^T \underline{\tilde{\theta}}_{ir}(0) \right] \\ &\quad + \frac{1}{2} \sum_{i=1}^N \left[ \rho^2 \int_0^T \underline{w}_i^T \underline{w}_i dt \right] \end{aligned} \quad (56)$$

is obtained.

Therefore, the  $H^\infty$  tracking equation (50) can be achieved and the proof is completed.

## 6. Simulation Results

This section presents four simulation examples to illustrate the effectiveness of the proposed control scheme. In the first example, a group of six agents with known dynamics as in (8) is considered. The second example presents the hexagonal formation of six partially unknown agents and an adaptive fuzzy logic system is used to approximate the unknown dynamics. This example proves the system stability under the proposed novel controller. In order to prove the

TABLE 1: Parameter specifications of hexagonal formation.

	$ i - j  = 1$	$ i - j  = 2$	$ i - j  = 3$	$ i - j  = 4$	$ i - j  = 5$
$d_{ij}$	1.0	1.7	2.0	1.7	1.0

TABLE 2: Agents initial positions.

Agent number	1	2	3	4	5	6
$x_0$	-2.5	+2.0	-1.0	+1.0	+2.0	+2.5
$y_0$	+1.0	-2.5	+1.0	-1.0	+2.5	-1.0

controller robustness, in the third example a white Gaussian noise is applied to all measured data and one of the agents is forced to be stationary and still the formation maintains its stabilizing performance. In the fourth example one of the agents is chosen as the leader with a constant velocity. It is shown that proposed controller is able to form a dynamic 2D moving hexagon which tracks the leader. All the simulation results are implemented in MATLAB with 0.01 secs as the stepsize.

The unique formation problem used in all five simulation examples is a 2D hexagon with unit radius defined by

$$F = \sum_{i=1}^5 \sum_{j=i+1}^6 \left( |z_i - z_j|^2 - d_{ij} \right)^2, \quad (57)$$

where  $d_{ij}$  is specified in Table 1.

In addition six random points in the 2D space are chosen to be the initial positions for six agents. These points are assumed to be fixed in all five numerical simulations (Table 2).

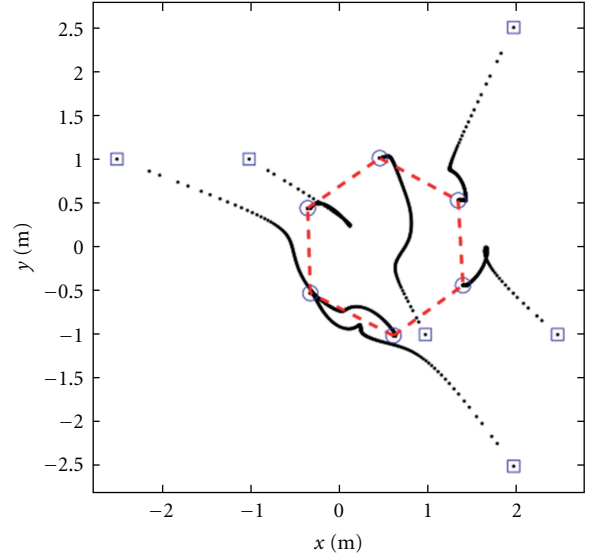
**6.1. Example I (Six Agents with Known Dynamics).** Consider a group of six mobile agents with known dynamic models. Based on general model represented in (8), the nonlinear dynamic of the  $i$ th robot is considered as

$$\begin{aligned} & \begin{bmatrix} 0.6 & 0 \\ 0 & 0.6 \end{bmatrix} \begin{bmatrix} \ddot{x}_i \\ \ddot{y}_i \end{bmatrix} + \begin{bmatrix} 0.15 & 0 \\ 0 & 0.15 \end{bmatrix} \begin{bmatrix} \dot{x}_i \\ \dot{y}_i \end{bmatrix} + \begin{bmatrix} 0.2 & 0 \\ 0 & 0.2 \end{bmatrix} \begin{bmatrix} \text{sgn}(\dot{x}_i) \\ \text{sgn}(\dot{y}_i) \end{bmatrix} \\ & = u_i, \end{aligned} \quad (58)$$

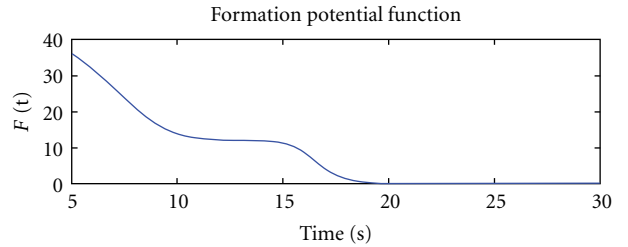
and after some manipulations we get

$$\begin{aligned} \begin{bmatrix} \ddot{x}_i \\ \ddot{y}_i \end{bmatrix} &= - \begin{bmatrix} 0.25 & 0 \\ 0 & 0.25 \end{bmatrix} \begin{bmatrix} \dot{x}_i \\ \dot{y}_i \end{bmatrix} - \begin{bmatrix} 0.33 & 0 \\ 0 & 0.33 \end{bmatrix} \begin{bmatrix} \text{sgn}(\dot{x}_i) \\ \text{sgn}(\dot{y}_i) \end{bmatrix} \\ &+ \begin{bmatrix} 1.66 & 0 \\ 0 & 1.66 \end{bmatrix} u_i. \end{aligned} \quad (59)$$

To give a solution for the formation problem, formation error is defined as (26) and the control law is designed based on (29), where  $k_1 = 15$  and  $k_2 = 4$ . Figure 3(a) shows the formation trajectory of six robots starting from initial



(a)



(b)

FIGURE 3: Hexagonal formation of six agents with known dynamics. (a) Formation trajectory. (b) Formation potential.

conditions (Table 2) to the final unit hexagon (57) in 30 secs and Figure 3(b) shows the potential value.

The first subfigure (Figure 3(a)) shows how smooth the controller guides all the agents to form the desired hexagon. This geometric formation does not have any fixed position or direction, and it will only be determined by the agents initial position.

The second sub-figure (Figure 3(b)) illustrates the potential decrement through the time. It is shown that the potential is forced to get stabilized in less than 20 secs and it will be shown that the settling time for next simulation examples will more than 20 secs.

**6.2. Example II (Six Agents with Partially Unknown Dynamics).** To verify the effectiveness of proposed method the same novel formation error and (26) are chosen, respectively. Consider a group of six agents with the same dynamic models as (59). However, to design the control law, the dynamic model of agents is assumed to be partially unknown (i.e.,  $C(\cdot)$  and  $g(\cdot)$  in (8) are unknown).

Therefore, six fuzzy logic approximators are designed to approximate the unknown dynamic, where each agent approximator just needs the current position and velocity of

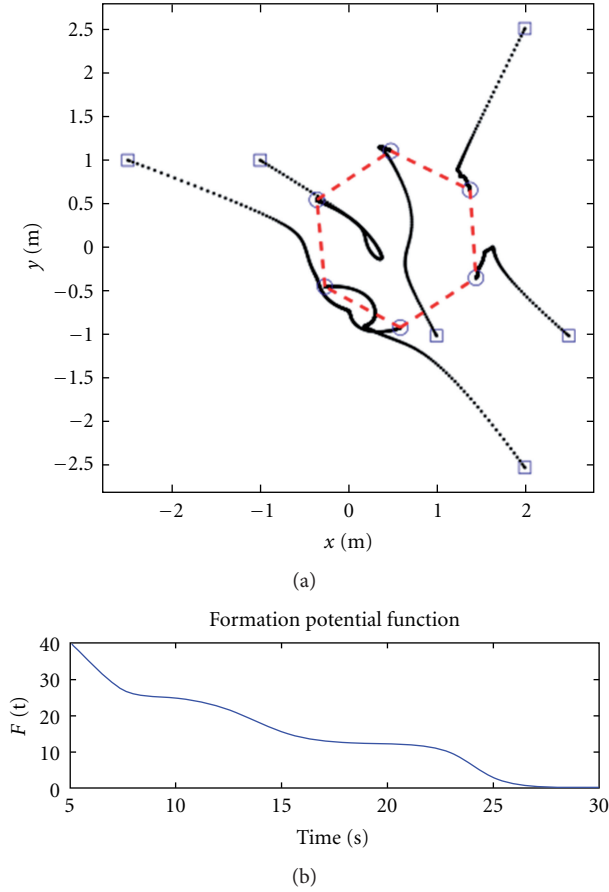


FIGURE 4: Hexagonal formation of six agents with partially unknown dynamics. (a) Formation trajectory. (b) Formation potential.

itself. Three Gaussian membership functions with unit variance are defined and all  $\theta$ s are initialized from zero vectors. The learning rate in (48) is set to  $\gamma = 15$  and the output of the fuzzy system is achieved by choosing singleton fuzzification, center average defuzzification, Mamdani implication in the rule base, and product inference engine [38].

Simulation results of the proposed adaptive fuzzy  $H^\infty$  technique with agents initial positions as shown in Table 2 are shown as following. The motion trajectory in the first 30 secs is illustrated in Figure 4(a) and the formation potential (57) is shown to be stabilized in Figure 4(b).

**6.3. Example III (Formation Problem in Presence of Measurement Noise and Agent Failure).** In this example the robustness of proposed controller in presence of measurement noise and agent failure will be proved. The proposed potential function (3) and gradient-based method proposed in Section 2 are able to obtain the exact formation even in the case of one agent failure. Therefore, in this example it will be shown that when Agent #3 ( $x_3(0) = -1, y_3(0) = +1$ ) is forced to be stationary with zero velocity, other agents move toward this agent to achieve the hexagon formation. In addition a white Gaussian noise with SNR = 20 db is applied to all the measured data. All of the model characteristics and controller

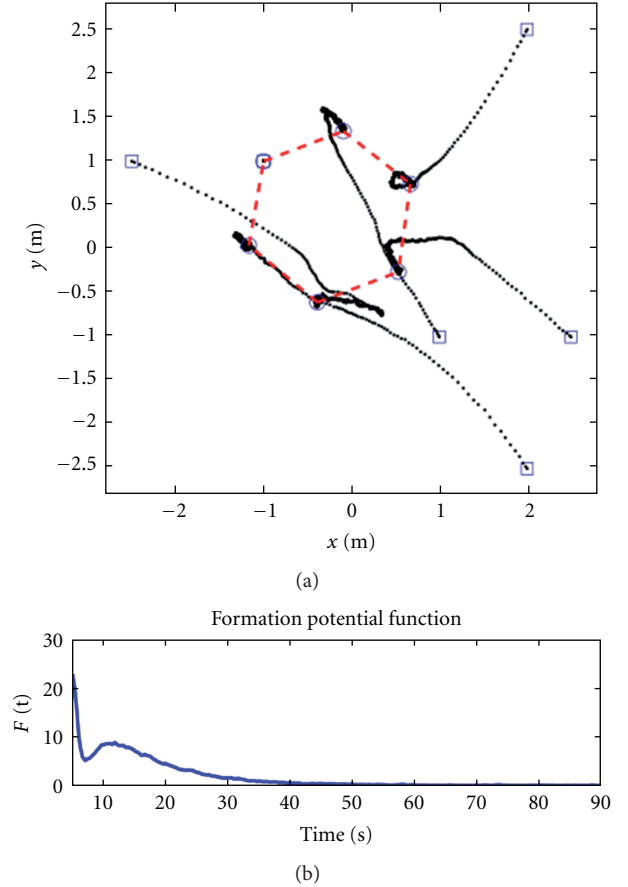


FIGURE 5: Hexagonal formation in presence of 20 db noise and one agent failure. (a) Formation trajectory. (b) Formation potential.

designs are the same as previous example in Section 6.2. Motion trajectory and formation potential (57) of the first 90 secs of simulation are shown in Figures 5(a) and 5(b), respectively.

**6.4. Example IV (Formation Problem While Tracking the Leader).** Previous example illustrated the good performance of formation stabilization, while agent failure (i.e., one agent remains stationary). However, the structure of potential function explained in (3) suggests to exempt one agent from the control law designed in (33), and let it move freely as the leader [8]. Therefore, to run a more general simulation than previous example where one agent was stationary, here one of the agents is chosen as the leader and moves with a constant speed to a predefined direction. Then it is anticipated that, after some transient formation, the agents position achieves the hexagon form in (57). All the problem parameters and controller design are the same as previous examples (i.e., (57), (59) and (42)). Agent #4 ( $x_4(0) = +1, y_4(0) = -1$ ) is chosen as the leader, with constant velocity as

$$\begin{aligned} \dot{x}_4 &= +0.030, \\ \dot{y}_4 &= -0.005. \end{aligned} \quad (60)$$

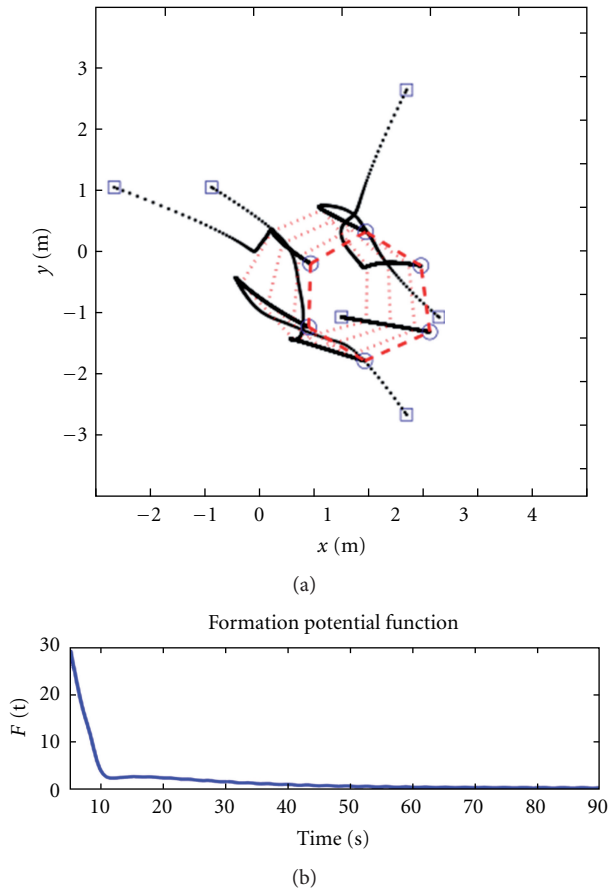


FIGURE 6: Moving hexagonal formation while tracking the leader. (a) Formation trajectory. (b) Formation potential.

The motion trajectory and formation potential (57) are shown in Figures 6(a) and 6(b), respectively.

Simulation results prove that by using the same control law as (33) even the moving formation can be achieved. It can be seen that the formation is achieved in about 70 secs; however, this numerical simulation contains negligible steady state error (Figure 6(b)).

## 7. Conclusion

In this paper, the formation control problem of a class of multiagent systems with partially unknown dynamics was investigated. On the basis of the Lyapunov stability theory, a novel decentralized adaptive fuzzy controller with corresponding parameter update law was developed and the stability of the system was proved even in the case of external disturbances and input nonlinearities. All the theoretical results were verified by simulation examples and good performance of the proposed controller was shown even in the case of agent failure, presence of measurement noise, and even moving formations.

## References

- [1] A. Badawy and C. R. McInnes, "Small spacecraft formation using potential functions," *Acta Astronautica*, vol. 65, no. 11-12, pp. 1783–1788, 2009.
- [2] L. E. Barnes, M. A. Fields, and K. P. Valavanis, "Swarm formation control utilizing elliptical surfaces and limiting functions," *IEEE Transactions on Systems, Man, and Cybernetics, Part B*, vol. 39, no. 6, pp. 1434–1445, 2009.
- [3] S. H. Kim, C. Park, and F. Harashima, "A self-organized fuzzy controller for wheeled mobile robot using an evolutionary algorithm," *IEEE Transactions on Industrial Electronics*, vol. 48, no. 2, pp. 467–474, 2001.
- [4] Y. Chung, C. Park, and F. Harashima, "A position control differential drive wheeled mobile robot," *IEEE Transactions on Industrial Electronics*, vol. 48, no. 4, pp. 853–863, 2001.
- [5] J. M. Lee, K. Son, M. C. Lee, J. W. Choi, S. H. Han, and M. H. Lee, "Localization of a mobile robot using the image of a moving object," *IEEE Transactions on Industrial Electronics*, vol. 50, no. 3, pp. 612–619, 2003.
- [6] M. J. Er and C. Deng, "Obstacle avoidance of a mobile robot using hybrid learning approach," *IEEE Transactions on Industrial Electronics*, vol. 52, no. 3, pp. 898–905, 2005.
- [7] D. Lee and W. Chung, "Discrete-status-based localization for indoor service robots," *IEEE Transactions on Industrial Electronics*, vol. 53, no. 5, pp. 1737–1746, 2006.
- [8] J. H. Reif and H. Wang, "Social potential fields: a distributed behavioral control for autonomous robots," *Robotics and Autonomous Systems*, vol. 27, no. 3, pp. 171–194, 1999.
- [9] S. Kato, S. Tsugawa, K. Tokuda, T. Matsui, and H. Fujii, "Vehicle control algorithms for cooperative driving with automated vehicles and intervehicle communications," *IEEE Transactions on Intelligent Transportation Systems*, vol. 3, no. 3, pp. 155–160, 2002.
- [10] B. A. White, A. Tsourdos, I. Ashokaraj, S. Subchan, and R. Zbikowski, "Contaminant cloud boundary monitoring using network of UAV sensors," *IEEE Sensors Journal*, vol. 8, no. 10, pp. 1681–1692, 2008.
- [11] R. Sepulchre, D. A. Paley, and N. E. Leonard, "Stabilization of planar collective motion: all-to-all communication," *Institute of Electrical and Electronics Engineers. Transactions on Automatic Control*, vol. 52, no. 5, pp. 811–824, 2007.
- [12] D. V. Dimarogonas and K. J. Kyriakopoulos, "Connectedness preserving distributed swarm aggregation for multiple kinematic robots," *IEEE Transactions on Robotics*, vol. 24, no. 5, pp. 1213–1223, 2008.
- [13] M. Proetzsch, T. Luksch, and K. Berns, "Development of complex robotic systems using the behavior-based control architecture iB2C," *Robotics and Autonomous Systems*, vol. 58, no. 1, pp. 46–67, 2010.
- [14] K. Peng and Y. Yang, "Leader-following consensus problem with a varying-velocity leader and time-varying delays," *Physica A*, vol. 388, no. 2-3, pp. 193–208, 2009.
- [15] H. Takahashi, H. Nishi, and K. Ohnishi, "Autonomous decentralized control for formation of multiple mobile robots considering ability of robot," *IEEE Transactions on Industrial Electronics*, vol. 51, no. 6, pp. 1272–1279, 2004.
- [16] M. Defoort, T. Floquet, A. Kökösy, and W. Perruquetti, "Sliding-mode formation control for cooperative autonomous mobile robots," *IEEE Transactions on Industrial Electronics*, vol. 55, no. 11, pp. 3944–3953, 2008.

- [17] C. C. Cheah, S. P. Hou, and J. J. E. Slotine, "Region-based shape control for a swarm of robots," *Automatica*, vol. 45, no. 10, pp. 2406–2411, 2009.
- [18] V. Gazi, "Swarm aggregations using artificial potentials and sliding-mode control," *IEEE Transactions on Robotics*, vol. 21, no. 6, pp. 1208–1214, 2005.
- [19] J. C. Doyle, K. Glover, P. P. Khargonekar, and B. A. Francis, "State-space solutions to standard  $H_2$  and  $H_\infty$  control problems," *Institute of Electrical and Electronics Engineers. Transactions on Automatic Control*, vol. 34, no. 8, pp. 831–847, 1989.
- [20] B. S. Chen, T. S. Lee, and J. H. Feng, "A nonlinear  $H_\infty$  control design in robotic systems under parameter perturbation and external disturbance," *International Journal of Control*, vol. 59, no. 2, pp. 439–461, 1994.
- [21] G. Willmann, D. F. Coutinho, L. F. A. Pereira, and F. B. Libano, "Multiple-loop H-Infinity control design for uninterruptible power supplies," *IEEE Transactions on Industrial Electronics*, vol. 54, no. 3, pp. 1591–1602, 2007.
- [22] K. H. Kwan, Y. C. Chu, and P. L. So, "Model-based  $H_\infty$  control of a unified power quality conditioner," *IEEE Transactions on Industrial Electronics*, vol. 56, no. 7, pp. 2493–2504, 2009.
- [23] R. Wang, G. P. Liu, W. Wang, D. Rees, and Y. B. Zhao, " $H_\infty$  control for networked predictive control systems based on the switched Lyapunov function method," *IEEE Transactions on Industrial Electronics*, vol. 57, no. 10, pp. 3565–3571, 2010.
- [24] A. G. Loukianov, J. Rivera, Y. V. Orlov, and E. Y. Morales Teraoka, "Robust trajectory tracking for an electrohydraulic actuator," *IEEE Transactions on Industrial Electronics*, vol. 56, no. 9, pp. 3523–3531, 2009.
- [25] B. S. Chen, C. H. Lee, and Y. C. Chang, " $H_\infty$  tracking design of uncertain nonlinear SISO systems: adaptive fuzzy approach," *IEEE Transactions on Fuzzy Systems*, vol. 4, no. 1, pp. 32–43, 1996.
- [26] L. A. Zadeh, "Fuzzy sets," *Information and Computation*, vol. 8, pp. 338–353, 1965.
- [27] X. D. Sun, K. H. Koh, B. G. Yu, and M. Matsui, "Fuzzy-logic-based V/f control of an induction motor for a DC grid power-leveling system using flywheel energy storage equipment," *IEEE Transactions on Industrial Electronics*, vol. 56, no. 8, pp. 3161–3168, 2009.
- [28] N. Yagiz, Y. Hacioglu, and Y. Taskin, "Fuzzy sliding-mode control of active suspensions," *IEEE Transactions on Industrial Electronics*, vol. 55, no. 11, pp. 3883–3890, 2008.
- [29] C. Cecati, F. Ciancetta, and P. Siano, "A multilevel inverter for photovoltaic systems with fuzzy logic control," *IEEE Transactions on Industrial Electronics*, vol. 57, no. 12, pp. 4115–4125, 2010.
- [30] F.-J. Lin and P.-H. Chou, "Adaptive control of two-axis motion control system using interval type-2 fuzzy neural network," *IEEE Transactions on Industrial Electronics*, vol. 56, no. 1, pp. 178–193, 2009.
- [31] P. Shahmaleki, M. Mahzoon, and B. Ranjbar, "Real time experimental study of truck backer upper problem with fuzzy controller," in *Proceedings of the World Automation Congress (WAC'08)*, Hawaii, USA, October 2008.
- [32] T. Das and I. N. Kar, "Design and implementation of an adaptive fuzzy logic-based controller for wheeled mobile robots," *IEEE Transactions on Control Systems Technology*, vol. 14, no. 3, pp. 501–510, 2006.
- [33] Z. Lin, B. Francis, and M. Maggiore, "Necessary and sufficient graphical conditions for formation control of unicycles," *IEEE Transactions on Automatic Control*, vol. 50, no. 1, pp. 121–127, 2005.
- [34] Y. Hu, W. Zhao, and L. Wang, "Vision-based target tracking and collision avoidance for two autonomous robotic fish," *IEEE Transactions on Industrial Electronics*, vol. 56, no. 5, pp. 1401–1410, 2009.
- [35] J. Ferruz, V. M. Vega, A. Ollero, and V. Blanco, "Reconfigurable control architecture for distributed systems in the HERO autonomous helicopter," *IEEE Transactions on Industrial Electronics*, vol. 58, no. 12, Article ID 5437249, pp. 5311–5318, 2011.
- [36] G. Cai, B. M. Chen, K. Peng, M. Dong, and T. H. Lee, "Modeling and control of the yaw channel of a UAV helicopter," *IEEE Transactions on Industrial Electronics*, vol. 55, no. 9, pp. 3426–3434, 2008.
- [37] E. Slotine and W. Li, *Applied Nonlinear Control*, Prentice-Hall, Englewood Cliffs, NJ, USA, 1991.
- [38] L. X. Wang, *A Course in Fuzzy Systems and Control*, Prentice-Hall, Englewood Cliffs, NJ, USA, 1997.
- [39] H. G. Tanner, A. Jadbabaie, and G. J. Pappas, "Flocking in fixed and switching networks," *Institute of Electrical and Electronics Engineers. Transactions on Automatic Control*, vol. 52, no. 5, pp. 863–868, 2007.



**Hindawi**

Submit your manuscripts at  
<http://www.hindawi.com>

